

# Refined Prediction of End Bearing through Multi-Level High Strain Dynamic Measurements

Ryan C. Allin, P.E., M.ASCE,<sup>1</sup> Frank Rausche, PhD., P.E., M.ASCE,<sup>2</sup>  
Brent R. Robinson, PhD., P.E., M. ASCE<sup>3</sup>

<sup>1</sup>Pile Dynamics, Inc., 30725 Aurora Rd, Cleveland, Ohio 44139; email: [rallin@pile.com](mailto:rallin@pile.com)

<sup>2</sup>Pile Dynamics, Inc., 30725 Aurora Rd, Cleveland, Ohio 44139; email: [frausche@pile.com](mailto:frausche@pile.com)

<sup>3</sup>Pile Dynamics, Inc., 30725 Aurora Rd, Cleveland, Ohio 44139; email: [brobinson@pile.com](mailto:brobinson@pile.com)

## ABSTRACT

High Strain Dynamic Testing (HSDT) has been used successfully as part of or the sole means of loading test programs on both driven pile and drilled foundations. Signal matching analysis of pile top force and velocity measurements allows for modelling of soil resistance and its distribution along the pile, determining not only the total static resistance, but also the end bearing component. While the estimation of total static resistance has been proven reliable with multiple published correlation studies performed, the accurate estimation of shaft resistance vs end bearing is limited. This limitation is caused by the lack of resolution of the measurements and relatedly, the difficulty of distinguishing between the end bearing and shaft resistance near the pile bottom. This ability is further complicated on drilled foundations due to the non-uniform nature of these foundation types. The best available means of improving the accuracy of the calculated end bearing - shaft resistance distribution is making additional measurements of force and velocity near the toe. The analysis of this data requires a multi-level signal matching approach.

This paper describes measurement and analysis techniques which were developed for the purpose of improving the resistance distribution predictions of HSDT. Three case studies are presented, where pile top and pile toe measurements in combination were taken on various foundation types which allowed for a more refined prediction of end-bearing through a multi-level analysis of the data at the pile toe and pile top. Limitations of this approach are also discussed.

## INTRODUCTION

Based on the initial dynamic testing research, performed over fifty years ago (Goble and Rausche, 1970), dynamic testing has provided a cost effective yet reliable means of predicting static soil resistance. Dynamic testing requires the application of an impact by a substantial mass (such as a pile driving hammer for driven piles, or a large drop weight) to cause a downward displacement thereby activating soil resistance. Upon impact a stress wave travels down the pile at a wave speed,  $c$ , dependent on the properties of the pile material. The measured force,  $F$ , and velocity,  $v$ , must stay proportional to one another by the impedance,  $Z$ , if the pile is uniform and there are no external forces acting on the pile.

The pile's impedance is defined as the product of the elastic modulus of the pile material,  $E$ , and the cross-sectional area of the pile,  $A$ , divided by the wave speed.

$$Z = \frac{EA}{c}$$

Any encounter with either a change in pile properties or soil resistance will cause an upward reflection of the stress wave. The travel time between the initial downward wave and the arrival of the upward wave from the pile toe for a pile with length,  $L$ , is  $2L/c$ . The time the stress wave's peak begins traveling down the pile to the sensors is referred to as  $t_1$ , and the arrival of the upward traveling wave at the sensors from the pile toe is referred to as  $t_2$ .

Because the activation of soil resistance occurs rapidly, the analysis requires the consideration of not only static resistance but also dynamic resistance. The total resistance is the sum of static plus dynamic resistance.

$$R_{Total} = R_{Static} + R_{Dynamic}$$

Dynamic resistance, being a function of pile velocity, must then be estimated through some means. If we consider the pile is impacted and a stress wave is sent down the pile, at some point, based on pile geometry and soil resistance, a reflected wave will return and thus the measured force,  $F_m$ , at the pile top would represent the sum of the downward force,  $F_{\downarrow}$  and upward force,  $F_{\uparrow}$ .

$$F_m = F_{\downarrow} + F_{\uparrow}$$

Separation of the downward force from the upward force is desirable as it allows separation of inputs (downward wave force) from reflections (upward wave force.) With force obtained from measured strain and the pile top velocity,  $v_m$ , obtained through integration of measured acceleration, the downward wave force as a function of time at a measurement point can be calculated as:

$$F_{\downarrow}(t) = \frac{(F_m(t) + v_m(t)Z)}{2}$$

And the upward wave force can be calculated as

$$F_{\uparrow}(t) = \frac{(F_m(t) - v_m(t)Z)}{2}$$

A closed-form solution, the Case Method (Rausche et al., 1985), allows for real time (i.e., during pile driving) prediction for each impact of mobilized bearing resistance through the selection of the Case damping value,  $J_C$ , where the static resistance can be calculated from the equation

$$R_{Static} = (1 - J_C)F_{\downarrow@t1} + (1 + J_C)F_{\uparrow@t2}$$

Two limitations to this simplified approach are the uncertainty of choosing an appropriate damping value and that it can only be used on uniform piles. The application of a closed-form solution when applied to drilled foundations becomes limited and therefore the user must resort to signal matching as the sole means of capacity assessment.

## **SIGNAL MATCHING**

Since its inception in 1969, the CAPWAP signal matching program (Rausche et al., 1985) has been routinely utilized as a standard practice for high-strain dynamic testing for capacity calculation. In contrast to a closed-form solution, the CAPWAP model breaks the pile into discrete segments and allows for modelling of static resistance, dynamic resistance, soil elasticity (quake) and unloading parameters for each soil segment. With the measured downward wave force as an input, initial soil model variables are assigned and then iteratively adjusted to produce a computed upward wave force which is then compared to the measured upward wave force. By minimizing the difference between calculated and measured wave force, the best fit soil model is determined and the static resistance can then be separated from the total resistance and used to develop a simulated load versus displacement curve.

## **RELIABILITY OF DYNAMIC TESTING**

Numerous correlation studies have been performed over the years demonstrating the reliability of static bearing resistance from dynamic measurement when compared to a static load test. Most notably, Likins and Rausche (2004) presented a correlation study including 303 cases with driven piles, drilled shafts and continuous flight augured (CFA) piles. Statistical results show that when given proper time considerations and both tests are run to failure, CAPWAP prediction over 303 cases shows a capacity ratio of ratio of CAPWAP prediction over static load test failure value of 0.98 with a coefficient of variation of 0.169 (Likins and Rausche, 2004).

Being a result of the standard signal matching analyses, the calculated end bearing, and shaft resistance distribution are generally part of a report documenting the results of a dynamic load test.

## **LIMITATIONS TO THE CAPWAP MODEL**

While signal matching of pile top measurements has shown to be a reliable means of capacity estimation, there are limitations to the accuracy and resolution of shaft resistance near the pile toe and end bearing. The near-toe shaft resistance and end bearing resistance can to some degree be interchanged in the analysis without a severe penalty to match quality. As an example, consider Figure 3 which is an installation record of the pipe pile of Case Study 1 below. It shows, as a function of time, pile top force,  $F$ , and pile top velocity,  $v$ , times  $Z$ . The third curve is the force in the upward traveling wave,  $F_{\uparrow}$ .

$F_{\uparrow}$  is an image of the sum of the shaft resistance forces. It begins to increase shortly after the time of impact, 35 ms. At that time, force and velocity begin to sharply increase reaching a first major peak at 36.3 ms. The rise time of this record,  $t_r$ , is, therefore, 1.3 ms. At time  $2L/c$  (twice the pile length divided by the wave speed) after the initial rise (35 ms), the toe reflected impact wave returns initiating a subsequent reduction in  $F$  and  $F_{\uparrow}$  and a relative increase in  $v$ . At the same time the effect of the increasing toe resistance is felt at the pile top. The rise time is typically also the time which it takes for a resistance force to get activated. In the example we would therefore expect that the bottom segment of the shaft resistance and the toe resistance will only be activated after time  $2L/c$  after the first peak ( $36.3 + 2L/c$  in Figure 3). The greater  $t_r$ , the slower is the activation of shaft resistance forces and the greater the time over which the reflected impact wave and the activation of shaft resistance near the toe and at the toe are superimposing. In fact, a case can be

made that the activation of end bearing is superimposing with the activation of shaft resistance occurring over a distance equal to

$$L_u = t_r \left( \frac{c}{2} \right)$$

In the present example, with  $c = 16.8$  ft/ms which is the wave speed for steel,  $L_u = 1.3 \left( \frac{16.8}{2} \right) = 10.9$  ft or roughly 2 soil segments in the CAPWAP analysis (the soil is commonly divided in 6.6 ft (2 m) segments).

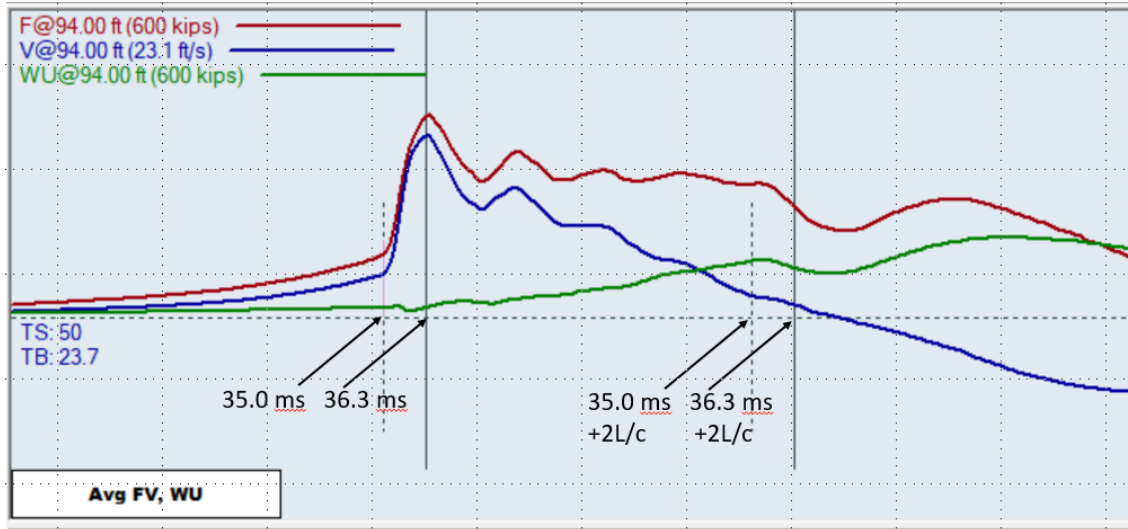


**Figure 1: High strain measurements during installation for Case 1.**

The thicker and softer a pile cushion protecting the pile top, the greater  $t_r$  and the greater, therefore, the uncertainty distance,  $L_u$ . Furthermore, soils which are more elastic, i.e., soils with relatively large shaft quakes take a longer time to activate the resistance which exacerbates the superposition problem of the resistance and reflected impact wave effects.

Estimates of end bearing on heavily cushioned piles will, therefore, benefit from additional information in the form of measurements near the pile toe. Of course, these measurements and their evaluation come at a high monetary cost and that is why standard signal matching is normally accepted as sufficiently accurate. Also, it should be emphasized that even with toe measurements, the accuracy of the end bearing calculation is not perfect depending on distance of the near-toe sensor(s) from the pile toe. Additionally, as for all strain measurements on concrete piles, calculated forces are hampered by an uncertain elastic modulus of the pile material and, for cast-in-situ piles, an uncertain cross-sectional area. Residual forces are an additional complication which tend to reduce the measured end bearing, which is a problem primarily for driven piles, but can also happen when cast-in-situ piles are tested with more than just a few impacts or after a static test.

In cases of uncertain pile geometry or elastic properties, to reduce the number of unknowns, either resistance distribution information must be obtained from soil borings or cross-sectional area versus depth must be known from installation records or Thermal Integrity tests. If that information

is not available, due to the large number of unknowns, the uncertainty in both instrumented static tests and dynamic solutions increases. Thermal testing is particularly useful because it allows for estimating an effective pile diameter versus depth.

### **MULTI-LEVEL METHODOLOGY FOR HIGH-STRAIN TESTING**

Multi-level instrumentation for a high-strain dynamic test is similar to the typical top instrumentation in that strain and acceleration measurements can be taken at multiple levels along the pile length to increase shaft resistance resolution. Previous experience with embedded dynamic strain and acceleration measurements has been conducted and reported as early as 1970 (Goble et al, 1970) and research has continued more recently (Tran et al, 2012).

The strain sensors should be resistive strain gages applied to ‘sister bars’ that can be tied to the longitudinal reinforcing steel. The sister bars must be long enough to assure sufficient bond to produce the same strain in the strain gage as in the surrounding concrete. Measurement of strain alone can be valuable as a sole means of force calculation versus depth, however, to separate dynamic effects and isolate static resistance at any given location, instrumentation must also include acceleration. With both strain and motion records available, signal matching can be done on any cross section as it would normally be done at the pile top, providing soil resistance and pile stress information for the pile portion below the point of measurement.

Embedded sensors should be placed at locations where soil layers are anticipated to change to high resistance, and most importantly, of course, above the pile toe to better define the end bearing. Consideration of end effects (non-uniform strain) and required bond length of the sister bars should also be considered in the length, number of, and placement of sensors. Multi-level signals may be continuously monitored for peak values of force, velocity, and stress.

### **CASE STUDY 1 – CLOSED ENDED, CONCRETE FILLED PIPE PILE**

A test program specified by the Ohio Department of Transportation required dynamic monitoring during the installation of four 12.75 inch closed end pipe piles with a wall thickness of 0.375 inches, one of which included instrumented static and multi-level dynamic load tests. This test pile’s length and required final pile penetration were 90.5 and 88 ft, respectively. The pile was filled with concrete after the initial installation, requiring the pile to be analyzed as a composite section.

A soil boring near the test pile location indicated primarily silt and clay throughout the depth of pile penetration. A 6 ft top layer was stiff to hard. The bottom 15 ft of pile penetrated into increasingly hard silt and clay layers containing traces of sand and gravel and reaching an SPT  $N_{60}$  value of 85 (Figure 2).

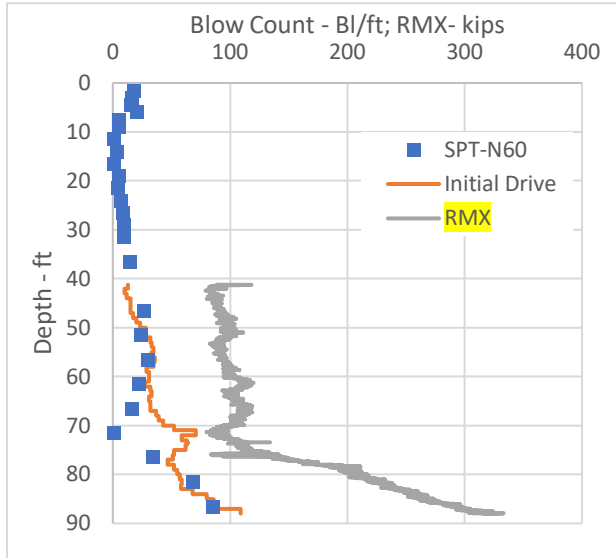


**Figure 2: SPT N60 blow counts, pile installation blow counts and Case method RMX resistance.**

The piles were dynamically monitored during initial installation while the pile was still an empty steel shell. The pile driving hammer was an ICE Model D19. Two strain transducers and two accelerometers were attached to the pile and monitored during pile installation according to ASTM D4945. Blow counts are shown in Figure 2 together with the Case Method Capacity Estimate with a  $J_c=0.9$  which is reasonable for cohesive soils. The final blow count was 109 blows/foot, corresponding to a set per blow of 0.11 inches.

Once the pile was installed, a one-inch diameter center bar was instrumented with the embedded sensors consisting of eight vibrating wire (VW) strain gages, three resistance strain gages (RS) and one piezoelectric accelerometer. The VW sensors were mounted by means of blocks

welded to the center bar while the RS sensors and accelerometer (Acc) had been attached to 36 inch-long, 0.5 inch diameter sister bars. The sister bars were wired to the center bar. The locations of external top sensors and embedded sensors are shown in Table 1. After inserting the center bar in the pipe pile, it was filled with concrete.

**Table 1: Instrumentation locations**

Elevation ft	Dist. to toe ft	Vib. Wire No.	Res. Strain Gage No.	Accelerometer
602.5	90.5	Pile Top	-	-
600.0	88.0	1	1, 2	1, 2
591.0	79.0	2	-	-
581.5	69.5	3	-	-
570.0	58.0	4	3	-
556.5	44.5	5	-	-
542.0	30.0	6	4	-
527.5	15.5	7	-	-
513.5	1.5	8	5	3
512.0	0.0	Pile Toe	-	-

The static load test was conducted nine days after initial drive and run to failure (defined at 562 kips). A 350-ton hydraulic jack applied the load. Pile top load measurements were obtained by both an electronic load cell and the jack pressure and from the VW No.1, providing a means of calculating the elastic modulus of the composite steel-concrete section for converting strain to force.

Two restrike tests were performed 13 and 23 days after initial installation using the D19 hammer. For pile protection, a cushion consisting of 2.25 inches of plywood was placed on the pile top. The penetrations per blow during the two restrikes were 0.05 and 0.02 inches, respectively; in other words, the blow counts were at or above practical refusal. Collection of embedded data occurred using two Pile Driving Analyzer® (PDA) systems. One PDA unit was connected to the standard set of top instrumentation which was attached to the steel shell, while a second PDA recorded the signals from the embedded RS and Acc instrumentation; also an additional pile top accelerometer was monitored by the second PDA for synchronizing the data. Figure 4 shows a restrike record with the top force, velocity and wave up on the upper graph and the same curves for the toe in the lower graph.

### **Analysis**

The analysis of the static test was done according to the Incremental Rigidity Method, IRM (Komurka and Robertson, 2020). This analysis provided static rigidity values, EA (elastic modulus times cross sectional area) for the composite steel-concrete pile sections between VW gage locations. Since the cross-sectional area is known in this case, the combined elastic modulus can be calculated from the combined EA value and from it, using steel area and modulus, the concrete modulus.

The top pile rigidity was checked by comparing the load cell readings with the internal strain readings yielding a composite static modulus of 6520 ksi. At the bottom, the IRM resulted in a combined modulus of 6900 ksi. For the static analysis, other pile sections had somewhat different rigidities and moduli. It is not unreasonable that the bottom concrete modulus of a cast-in-place pile is higher than at the top modulus considering the higher concrete pressure during curing at the

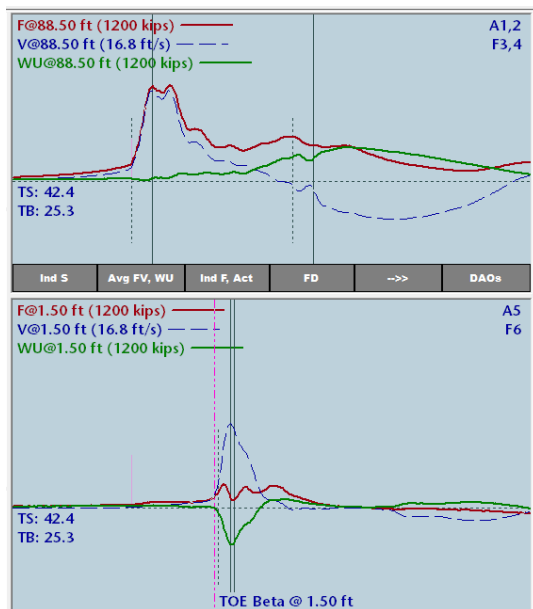


**Figure 3: PDA display of force, velocity and wave-up force at the pile top (88.5 ft) and bottom (1.5 ft).**

pile toe. The combined dynamic modulus, calculated from the time of stress wave return was 7550 ksi,. Considering that the static combined modulus was approximately 6% higher at the toe than at the top, it is possible that the dynamic modulus at the pile toe had a correspondingly higher value.

CAPWAP analysis of an end of driving record yielded a total resistance of 365 kips with a calculated end bearing component of 260 kips. At a maximum pile top displacement of 2.5 inches the static load test reached a maximum load of 562 kips at top and 211 kips 1.5 ft above the toe. The 211 kip force may be extrapolated to 186 kips of end bearing, assuming the resistance was uniform from VW 7 to the toe.

CAPWAP analyses were also performed for one blow each of the end of driving and the two restrikes. All analyses were performed using CAPWAPs Residual Stress Analysis. Normally CAPWAP analyses determine both end bearing and shaft

resistance values. However, if the end bearing is known, it can be imposed as a fixed boundary value at the pile bottom and the analysis has one less unknown. In the present case the different end bearing values, including the static and dynamic toe measurements, were tried to investigate the sensitivity of the match quality to a change of end bearing. In all cases the total pile capacity predicted by the signal matching analysis did not change.

Dynamic test results performed for the 13 and 23 day restrikes indicated capacities of 553 kips, and 604 kips, respectively, indicating continuing capacity gain due to set-up in the silty and clay soils. A CAPWAP analysis performed on the toe measurements resulted in a static end bearing value of 150 kips. Static and dynamic results are summarized in Table 2.

**Table 2: Results from static test and dynamic analyses**

Test	Total Resistance (kips)	End Bearing (kips)	Set per Blow (inch)	Top Max. Force (kips)	Top Max. Transfd. Energy (kip-ft)
Initial Drive	347	260	0.11	413	26.3
SLT	562	186	-	-	-
13 day Restrike	553	150*	0.05	693	21.5
23 day Restrike	604	150*	0.02	683	23.8

\*Based on dynamic toe measurements

### Match Sensitivity

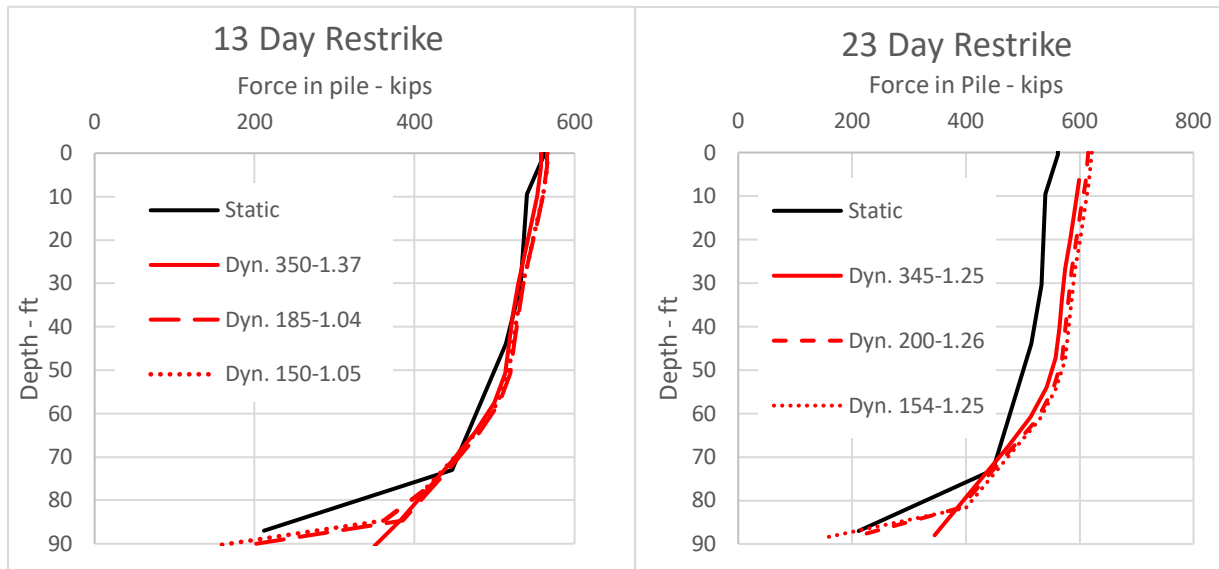


**Figure 4: Load transfer for static test (at 9 day) and dynamic signal matching with different end bearing values and match qualities**

The load transfer curves (Figure 5) were obtained by signal matching analysis from sensors near the pile top for both 13 (23) day restrikes with modelled CAPWAP end bearing values of 350, 185 and 150 (350, 200 and 150) kips and placing the difference between 350 and the lower end bearing values at the bottom shaft segment. The force at the nearest-to-toe shaft segment was plotted 3.3



ft (1/2 soil segment length) above the toe at the center of the nearest-to-toe segment length. Obviously, the resulting load transfer curves are not vastly different and suggest that it is difficult to distinguish between end bearing at the pile toe and the shaft resistance immediately above the toe. Match qualities, shown in the legend, are roughly defined as the average percentage difference between the absolute values of computed and measured wave-up force. The Match qualities are indicated in the legend with 1.04 being the optimum for the 185 kip analysis. The difference in match qualities is remarkably low and it is possible to identify 350 kips as the correct value. With such an insensitivity of the match the direct measurement of the toe resistance is of benefit; however, it does not completely solve that problem because of the necessary distance of the bottom force measurement from the pile toe.

Load displacement curves are shown in Figure 6 including the 3 different results from the 13 day restrike, which is closest to the 9 day static test. Regardless of the assumed end bearing value, the three simulated static load test curves are practically indistinguishable. For the measured dynamic toe load a displacement was calculated based on the load transfer curves of Figure 5.

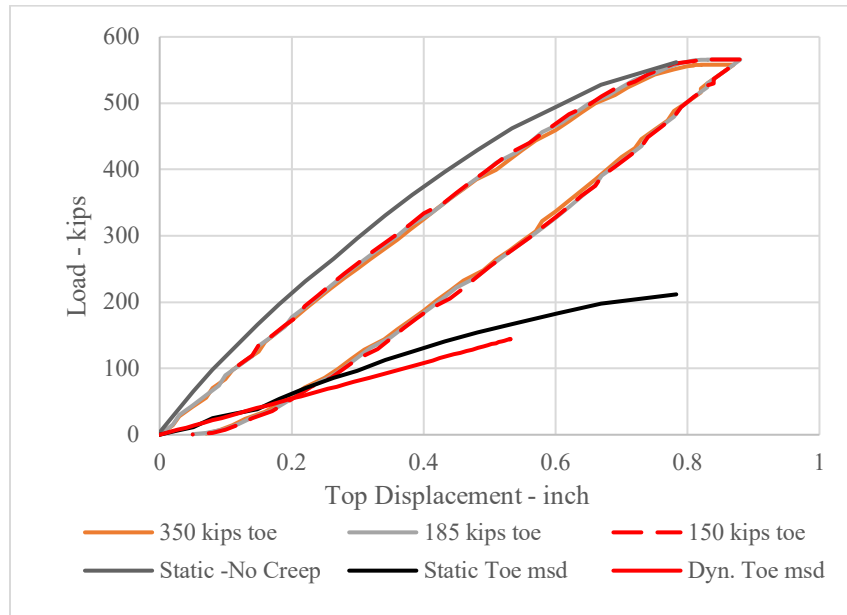


**Figure 5: Load vs displacement for static test and dynamic analyses**

## **Residual stress effects**

Loading a pile, either statically or dynamically, invariably leads to residual or locked-in stresses in the pile during pile unloading for piles subjected to both shaft resistance and end bearing. , Because the pile rebounds once the load is removed, the shaft resistance changes sign and tends to keep the pile in compression. Large numbers of hammer blows, driving interruptions, temperature and humidity changes, all can make the determination of the residual force by direct measurement very difficult. Commonly therefore, it is assumed that, when static loading begins or the next hammer blow is imminent, all forces in the pile and soil are zero. Residual stresses do not affect the total capacity calculated by signal matching analysis; they tend, however, to reduce the apparent end bearing and increase the apparent shaft resistance. These differences are generally insignificant for relatively rigid piles, e.g., concrete piles or short piles, but can be significant for slender piles of low rigidity. The residual effect has been studied by Holloway, 1978 and was included in the wave equation analysis, GRLWEAP (Hery, 1983, PDI, 2010), and the CAPWAP program (PDI 2014) as an analysis option. In the

**Table 3: CAPWAP residual force table for the 13 day restrrike**

RESIDUAL FORCE TABLE					
Soil Sgmt No.	Dist. Below Gages ft	Pile Residual Forces kips	Pile Stress ksi	Soil Residual Forces kips	Displ. in
Pile Top					0.03
1	6.8	0.4	0.00	-0.4	0.03
2	13.6	0.9	0.01	-0.5	0.03
3	20.4	1.3	0.01	-0.4	0.03
4	27.2	1.6	0.01	-0.3	0.03
5	34.0	1.8	0.01	-0.2	0.03
6	40.8	1.9	0.01	-0.2	0.03
7	47.7	2.1	0.02	-0.2	0.03
8	54.5	2.7	0.02	-0.6	0.03
9	61.3	4.1	0.03	-1.4	0.03
10	68.1	6.2	0.05	-2.1	0.03
11	74.9	9.0	0.07	-2.7	0.03
12	81.7	12.2	0.10	-3.2	0.03
13	88.5	15.0	0.12	-2.8	0.03
Toe				15.0	

present case, the residual force at the pile toe was estimated by performing an additional signal matching analysis with residual stresses. Table 3 shows the resulting residual forces in the pile. It should be mentioned that slightly better match qualities were achieved with residual stress analyses than with standard analysis.

## **DISCUSSION OF CASE 1**

The dynamic toe measurements aided in the analysis of the dynamic top data which, in this case, was very insensitive to toe resistance changes. This insensitivity is primarily attributed to the fact that the shaft resistance was concentrated near the pile toe. The reason for the dynamic toe resistance being lower than the static resistance is unknown but may be attributed to three potential causes: (a) the toe elastic modulus was likely approximately 6% higher at the toe, (b) the residual stresses may have made a 10% difference and (c) the dynamic restrrike tests encountered refusal and thus generally underpredicts the end bearing.

## **CASE STUDY 2 – DRILLED SHAFT**

Dynamic testing was conducted on a 42” diameter drilled shaft installed to a length of 70 ft. Embedded accelerometers and pairs of sister bars with resistive strain sensors (Figure 8) were installed 2 feet above the toe with strain sensors additionally installed at 28 and 48 ft above the

pile toe. An additional externally mounted accelerometer was installed near the pile top to trigger the embedded sensors. Pile top measurements were collected using a force transducer (Figure 10).

Both thermal integrity profiling (TIP) and cross-hole sonic logging (CSL) were used to evaluate integrity. Thermal results indicated a shaft free of defects with all cross-hole profiles concurring (Figure 10) and TIP additionally indicated the concrete cover was fairly uniform with depth except for a high temperature zone (indicating a local bulge), located 15 to 25 ft below top at one side of the pile (Figure 10).



**Figure 6: Resistive strain sensor and accelerometer are attached onto the reinforcement cage.**

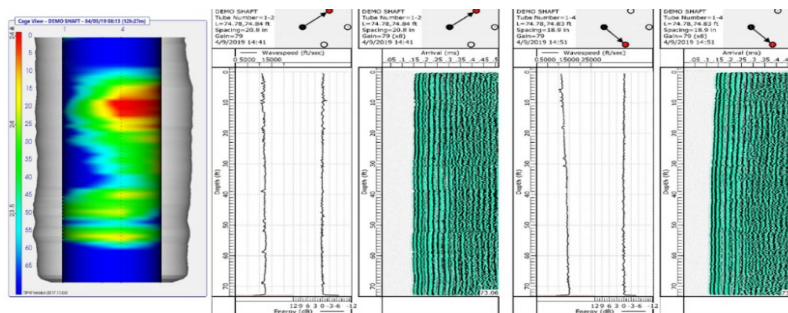


**Figure 7: Thermal integrity profile (left) and two of six CSL scans (right).**

Dynamic testing was performed by applying four impacts to the pile utilizing a 16 ton drop hammer (Figure 10). Drop heights ranged from 0.5 ft to 3.0 ft with permanent pile displacement not exceeding 0.05 inches per blow.



**Figure 8: The crew is setting the drop height of the 16-ton ram; the force transducer is placed between the red ram and the pile top.**

Signal matching performed from measurements taken only at the top indicated a total static resistance of 1705 kips with 1280 kips on the shaft and 425 kips at the toe (Table 4). The analysis was then repeated for all four impacts using signal matching at the toe and using the toe resistances calculated in that manner in the pile top analyses. The maximum capacity calculated was 1500 kips with 1200 kips of resistance on the shaft and 300 kips of end bearing.

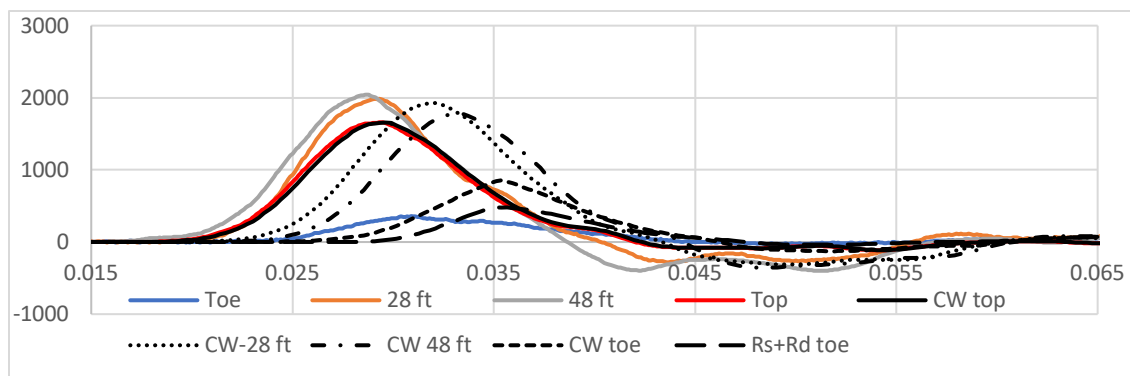


**Figure 9: Measured force and resistance curves plotted with time at various instrumentation levels.**

**Table 4: Case 2 summary of CAPWAP results**

CAPWAP Blow	Set/Blow inches	Total kips	Toe kips
1	0.00	700	121
2	0.00	1000	179
3	0.02	1549	263
4	0.05	1500	300
4*	0.05	1705	425

\*-Using top measurements only

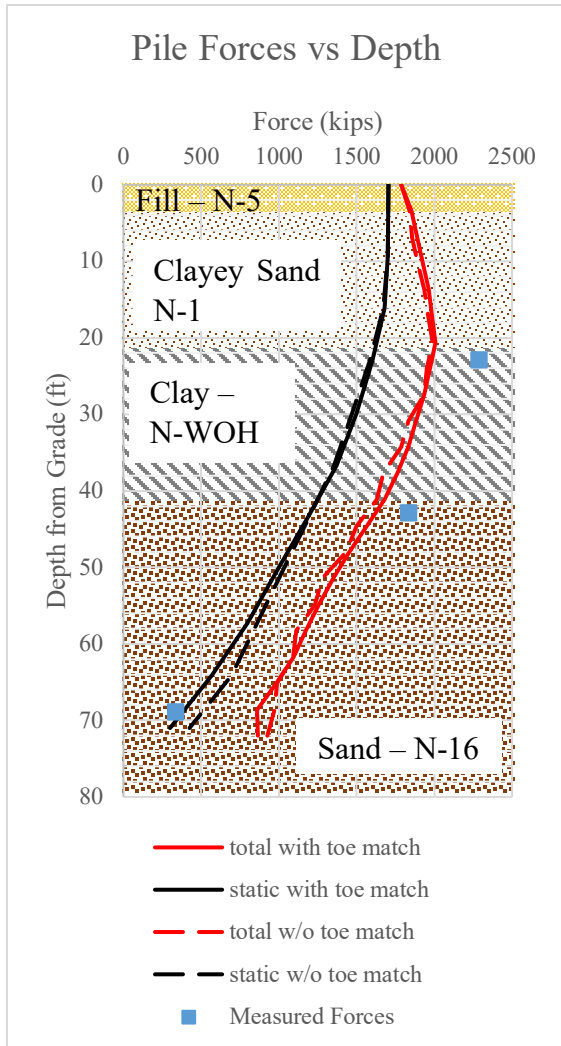


**Figure 10: Case 2 calculated forces at predicted capacity from signal matching**

Profiling (TIP) during curing and low-strain integrity testing (PIT) once the grout had hardened. Calculated pile shapes from both integrity methods are depicted in Figure 14. They did not indicate any detectable anomalies except that the pile was apparently oversized at the top and that the shape gradually reduced to the nominal diameter at a depth of 25 ft.

Measurements were collected over seven impacts from a 12-ton ram. Drop heights varied from 0.5 to 4 ft with permanent pile displacement per blow varying from 1/16" up to 3/4" for the final impact indicating that the soil resistance was fully mobilized. The third blow, with a drop height of 1.5 ft and a set of 3/16" was selected for analysis. CAPWAP analysis based solely on top measurements indicated a total resistance of 500 kips with

The calculated (dotted and dashed lines) and the measured (solid lines) force – time histories indicate highest peaks of respectively 1928 and 2038 kips, 48 ft above the toe. This observation is consistent with effects of wave superposition for a pile with high resistance in the lower part of the pile. In the static case, where dynamic superpositions do not occur, the measurements would show monotonically decreasing force values from top to toe.

### CASE STUDY 3 – PARTIAL DISPLACEMENT PILE

The third case study utilizes the embedded sensors attached to the center bar of a 16" (40 cm) partial displacement pile. The pile was installed with a length of 66 ft plus a one-foot buildup above existing grade to facilitate dynamic testing. The grout volume was 125 percent of theoretical. Nine-day compression testing of the concrete indicated strengths of around 7,000 psi. Strain measurements were placed at measurements of 1 foot, 11 feet, 33 feet and 60 feet above the pile toe with accelerometers placed both at the 1 foot and 60 foot level on a center bar (Figure 13).

During installation, the pile was tested using Thermal Integrity



**Figure 11: Center bar instrumented with sister bar strain sensor and Thermal Wire cable.**

445 kips of shaft resistance and 55 kips of end bearing. Signal matching at the toe indicated an end bearing of 75 kips. The calculated resistance distributions from static and total forces are shown in Figure 15 together with a simplified representation of the soil profile.

## CONSIDERATIONS AND LIMITATIONS

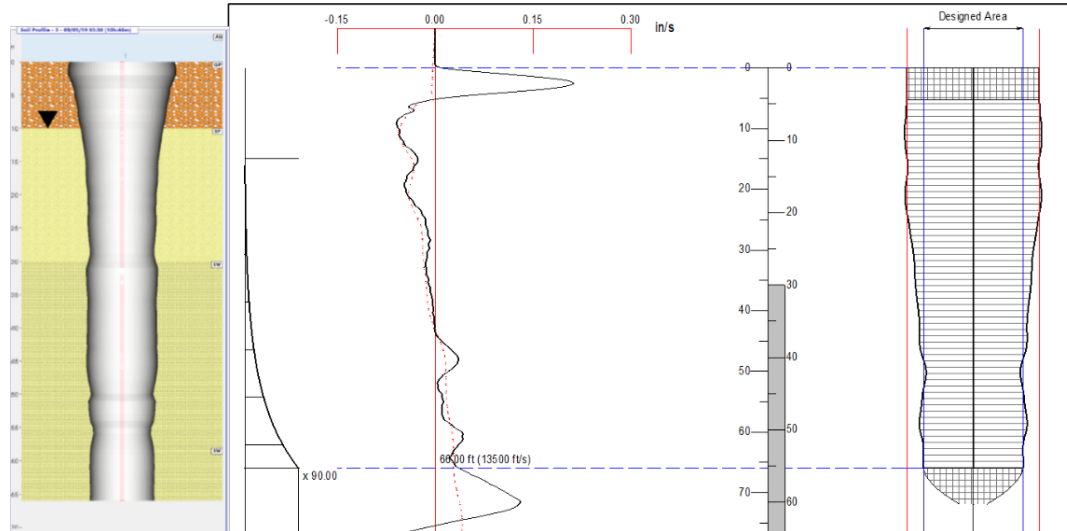


**Figure 12: Thermal Integrity results (left) and profile analysis from low strain testing.**

In all three cases presented in this paper, total static resistance was not drastically affected by the refined analysis using dynamic toe measurements of force and velocity. However, in instances where load distribution is of concern, multi-level instrumentation offers an additional tool in determination of load transfer for generally greater confidence in the accuracy of the results. Unfortunately, both toe dynamic measurements and analyses carry additional sources of errors, such as uncertainty of pile rigidity and residual stresses. The actual static resistance present at the toe may be higher due to preloading conditions from residual stresses built up in the pile through multiple impacts. Therefore, static end bearing resistance may be underpredicted (and shaft resistance overpredicted) unless those forces are added back in through some analysis. The CAPWAP residual stress analysis option includes such a correction. Unfortunately, direct residual stress measurements are complex and as of now cannot be performed easily and accurately. Strain transducers and accelerometers that must be cast into a pile add additional cost to a dynamic test, although still generally well below the cost of a comparable instrumented static load test.

## ACKNOWLEDGEMENTS

The authors gratefully acknowledge the contributions of Ben White, GRL Engineers, Inc. who took the Case 1 data; the Ohio Department of Transportation for releasing the Case 1 data for publication; Scott Webster, GRL Engineers, Inc. and Scott Wall, Atlantic Testing for Case 2 and Alex Ryberg, GRL Engineers, Inc. for doing the dynamic testing in Case 3.

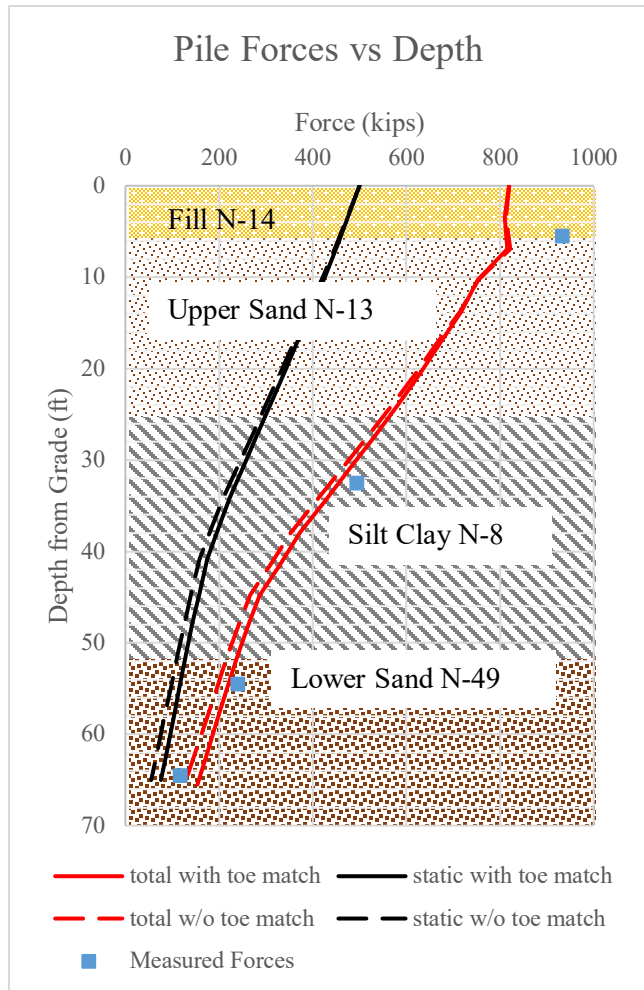


**Figure 15: Pile forces shown vs. depth with soil information.**

Method. ASCE GeoCongress 2020, Minneapolis, MN, Submitted.

Likins, G., Rausche, F. (2004) *Correlation of CAPWAP with Static Load Tests*, Proceedings of the Seventh International Conference on the Application of Stresswave Theory to Piles, Selangor, Malaysia, pp 153-165

Tran, Khiem & McVay, Michael & Herrera, Rodrigo & Lai, Peter. (2012). Estimating static tip resistance of driven piles with bottom pile instrumentation. *Canadian Geotechnical Journal*. 49. 381-393. 10.1139/t2012-001.

Rausche, F., Goble, G., Likins, G. | (1985). *Dynamic Determination of Pile Capacity*, ASCE Journal of Geotechnical Engineering, Vol. 111, No. 3, Reston, VA, pp 367-383; 1985

## REFERENCES

ASTM D4945-17 ; <http://www.astm.org/cgi-bin/resolver.cgi?D4945-17>

Goble, G., Rausche, F. (1970) "*Pile Load Testing by Impact Driving*," Highway Research Record No. 333, Washington, D.C., pp 123-129

Goble, G., Rausche, F., Moses, F. (1970) "*Dynamic Studies on the Bearing Capacity of Piles*"; Phase III Volume II Report No. 48 Case Western Reserve University, Cleveland, OH

Hery, P., (1983), "*Residual Stress Analysis in WEAP*," Master's Thesis, Department of Civil, Environmental, and Architectural Engineering, University of Colorado

Holloway, D.M., Clough, G.W., and Vesic, A.S., (1978), "*The Effect of Residual Driving Stresses on Pile Performance Under Axial Loads*," OTC 3306.

Komurka, V.E., & Robertson, S. (2020). Results and Lessons Learned from Converting Strain to Internal Force in Instrumented Static Loading Tests Using the Incremental Rigidity